ISLAMIC UNIVERSITY OF TECHNOLOGY (IUT)

NUMERICAL INVESTIGATION OF MASS INJECTION APPROACH FOR MITIGATION OF EROSION ON PROPELLER FROM CAVITATION

B.Sc. Engineering (Mechanical) THESIS

BY

NASIMUL ESHAN CHOWDHURY
STUDENT NO: 141440
Department of Mechanical and Chemical Engineering
Islamic University of Technology (IUT)

NOVEMBER 2018

NUMERICAL INVESTIGATION OF MASS INJECTION APPROACH FOR MITIGATION OF EROSION ON PROPELLER FROM CAVITATION

BY

NASIMUL ESHAN CHOWDHURY
STUDENT NO: 141440

A THESIS PRESENTED TO THE DEPARTMENT OF MECHANICAL AND CHEMICAL ENGINEERING OF ISLAMIC UNIVERSITY OF TECHNOLOGY DHAKA IN PARTIAL FULFILMENT OF THE REQUIREMENT FOR THE AWARD OF DEGREE FOR

BACHELOR OF SCIENCE (B. Sc.) IN MECHANICAL ENGINEERING

NOVEMBER 2018

Candidate's Declaration

It is hereby declared that this thesis has not been submitted elsewhere for the award of any degree or diploma.

Signature of the Candidate

_____

Nasimul Eshan Chowdhury
Student No: 141440
Department of Mechanical and Chemical Engineering (MCE)
Islamic University of Technology (IUT), OIC
Board Bazar, Gazipur
Dhaka, Bangladesh.

Signature of the Supervisor

_____

Dr. Arafat Ahmed Bhuiyan
Associate Professor
Department of Mechanical & Chemical Engineering (MCE)
Islamic University of Technology

Signature of the Head of the Department

_____

Prof. Dr. Md. Zahid Hossain
Head, MCE Department
Department of Mechanical & Chemical Engineering (MCE)
Islamic University of Technology

Acknowledgements

We would like to begin by saying Alhamdulillah and grateful to Almighty Allah who made it possible for us to finish this work successfully on time. Equally say a big thank you to our supervisor Dr. Mohammad Ahsan Habib, Associate Professor, Department of Mechanical and Chemical Engineering, IUT for all his support, ideas about experiments, discussions, time and for explaining so patiently the hard topics and checking this thesis and papers above all his care and concern. These will ever remain in our memory. Thanks to our examiners for their constructive ideas, suggestions and double checking our work.

Table of Contents

Table of Figures

Abstract

Cavitation in marine propeller is a common phenomenon and mitigate it is a demanding issue. In this regard, many studies have been carried out and some solutions have already been proposed. In fact, some of them are already in use. Air injection technique can be a new approach to this prevailing problem. The main focus of the current study is to construct a feasible numerical model that could suffice the approach and eventually use the model to investigate the effectiveness of this method. For this novel purpose, the k-ω SST turbulence model with the curvature correction and the Zwart cavitation model have been applied on the commercial CFD Code ANSYS. The combined model has been applied on a modified INSEAN E779a propeller. In case of light weight expandable mass, the method has been found very appealing. Besides, the model is robust enough to encompass the complexities of the cavitation phenomenon.

Introduction

A marine propeller is normally fitted to the stern of the ship where it operates in water that has been disturbed by the ship as it moves ahead. A propeller that revolves in the clockwise direction (viewed from aft) when propelling the ship forward is called a right hand propeller. When a propeller is moved rapidly in the water then the pressure in the liquid adjacent to body drops in proportion to the square of local flow velocity. If the local pressure drops below the vapor pressure of surrounding liquid, small pockets or cavities of vapor are formed. Then the flow slows down behind the object and these little cavities are collapsed with very high explosive force. If the cavitation area is sufficiently large, it will change the propeller characteristics such as decrease in thrust, alteration of torque, damage of propeller material (corrosion and erosion) and strong vibration excitation and noise.

During recent year's great advancement of computer performance, Computational Fluid-Dynamics (CFD) methods for solving the Reynolds Averaged Navier-Stokes (RANS) equation have been increasingly applied to various marine propeller geometries. While these studies have shown great advancement in the technology, some issues still need to be addressed for more practicable procedures. These include mesh generation strategies and turbulence model selection. With the availability of superior hardware, it becomes possible to model the complex fluid flow problems like propeller flow and cavitation.

For many years, propellers were predicted using the lifting-line theory, where the blade was represented by a vortex line and the wake by a system of helicoidal vortices. With the advent of computers, numerical methods developed rapidly from the 1960s onwards.

Cavitation erodes surface of the blades and these rough surfaces increase turbulences, which eventually decreases propeller efficiency [1]. Like boiling, cavitation is a phase changing process. But, the basic difference is that at boiling phase changes due to external heat addition at constant temperature; where at cavitation the phase changes due to drop of pressure below to the vapour pressure [2]. The cavitation occurs at roughly constant temperature, by decreasing the pressure (p) below the saturated vapour pressure (p_v), unlike the boiling, where the temperature is been raised to saturation temperature. The difference in the surrounding

pressure and the saturated vapour pressure is called the tension (Δp) and the magnitude at which cavitation initiates, is called the tensile strength of the liquid (ΔpC) [2].

Normally in two ways the cavitation is formed. The thermal motion within the liquid causes temporary microscopic voids, causing pressure drop and forming the nuclei for the cavitation bubbles. This formation is called 'homogeneous nucleation'. However, the most common type of formation is the 'heterogeneous nucleation', which is caused from the wake and the sudden pressure drop at the junction of the liquid and a solid boundary. Moreover, bubbles also form from the gasses, dissolved in the liquid. In water, micro bubbles of air seem to persist almost indefinitely and are almost impossible to remove completely [2]. In a typical marine various types of cavitation occur, as shown in Figure 1 [3]. In conventional propellers, the dominant type of cavitation is leading edge back cavitation, which forms on the suction side and detaches from the leading edge. On the other hand, midchord cavitation is the cavity that detaches from the leading edge [3]. Sheet cavitation and tip-vortex cavitation are responsible for vibration, particularly in the region, close to the hull plating above the propeller.

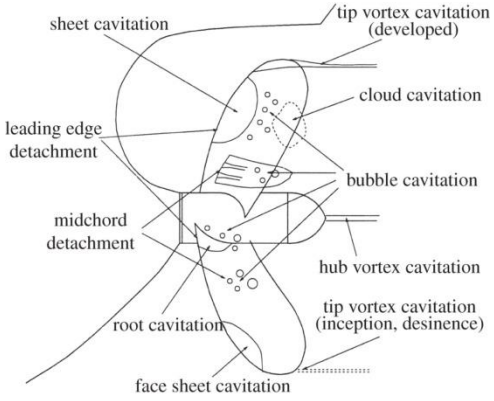

Figure 1: Various types of cavitation

However, the break-up of sheet cavitation and blade root cavitation cause serious erosion damage, as the cavities implode close to the material surface [4]. Having pressure difference between the contents of the cavity (vapour pressure) and the surrounding, the sheet and the vortex cavitation contain potential energy. This potential energy is converted to kinetic energy due to steep gradient of spatial pressure or temporal pressure. At a certain moment, the kinetic energy of the surrounding fluid increases to a point that shock waves occur, at the final stage of the collapse of the cavity. At this stage, the local pressure reaches up to 10 000 times of atmospheric pressure and local temperature rises up to 800 K [4]. Thus, the study focuses mainly on the mitigation of these two types of cavitation, by means of mass injection, similar to the study of T. M. Pham et al [5].

Many researches have been conducted on the palliation of propeller cavitation problem [1, 6, 7]. In case of cavitation reducing propeller design, the research of Brenden Epps et al [8], Sakir BAL [9] are worth mentioning. Moreover, the modified CLT propellers design of Stefano Gaggero et al [10] has given an outstanding reduction of the sheet cavity bubbles. Surface piercing method is a way to reduce cavitation [11]. The experimental study of Derek Peterson on this method [3], revealed that about 3-5% energy is lost if the propeller shaft is parallel to

the flow. Applying RANS simulation using VOF method, Yari and Ghassemi [11] has developed a convincing numerical model to facilitate economic studies on piercing technique. Regarding, the numerical analysis, H.Yu et al [12] has validated the compressible fractional step method for future studies. Similar validation studies have been conducted by Nobuaki Sakamoto et al [13], Gaggero et al [14] , Chao et al [15], Naz Yilmaz et al [16], Jian Hu et al[17] and Wu et al [18].

Mass injection approach is not so popular, as compare to other mitigating techniques [19, 20]. Moreover, there are very less studies on the issue [5, 21-24]. Among them, the study of G. L. Chahin et al [25] on reducing tip vortex cavitation by incompressible fluid injection, seems to be the pioneer to others on the topic. Subsequently, R. E. A. Arndt et al [23] studied on gas injection on blade surface. Afterwards, Knud Thomsen [21]contributed further on this concept. Later on, Jeung Lee et al [24] studied on mitigating cavitation from reflected wave from air-bubble layer. The study of Jeung-Hoon Lee et al [22] on air-filled rubber membrane in reducing hull exciting pressure and study of Chang-Sup Lee et al [26] on the effectiveness of water injection, found to be very demanding .

For a long time, numerical simulations of cavitating flow are solved with Reynolds-averaged Navier–Stokes (RANS) turbulence models. For example, Watanabe et al. [15] simulated the unsteady cavitation on a propeller based on a RANS turbulence model and the Singhal cavitation model with the use of the commercial software FLUENT. The cavity shape and pressure fluctuations they predicted on the blade surfaces were fairly consistent with the obtained measurements. The application of the CFD (computational fluid dynamics) to the cavitating flow around a propeller in a non-uniform ship wake was discussed by Nobuhiro et al. [15], who concluded that the RANS simulation could generate valuable information for judging erosion risk but its predictive accuracy and numerical stability are insufficiently good. Ji et al. [15] numerically simulated the propeller cavitation with the use of a SST turbulence model, a mass transfer cavitation model, and a sliding mesh approach; the predicted evolution of cavity and the pressure fluctuations on a propeller is in good agreement with experimental results. Furthermore, RANS turbulence models have been widely used in the numerical simulation of cavitation flows around other objects underwater [15]. Given that RANS turbulence models smooth a number of details of the turbulent movement, these methods has some limitations when simulating the effect of transient cavitation pulsation, whereas large-eddy simulation (LES) methods have performed better in this case. LES methods are designed to simulate large-scale movements of unsteady vortex structures to more accurately simulate the transient characteristics of turbulence. In recent years, LES turbulence models are used to numerically simulate cavitation flow and achieved some progress, however, research on propeller cavitation is very limited. For example, Bensow and Bark [15] simulated unsteady cavitating flows around an INSEAN E779A propeller by implicit LESs. They predicted some important cavitation mechanisms, which were useful in assessing cavitation erosion, proved the validity of the method, and pointed out that the LES of cavitation still needs further development and exploration. In addition, Lu et al. [15] adopted both LES and RANS simulation to simulate the cavitating flow on a marine propeller, and compared simulation results with experimental results. They found that more refined bubble and vortex structures

have been obtained in the LES-based simulation than in the RANS-based simulation. Then Lu et al. [15] simulated the cavitating flow around two highly skewed propellers operating in open water and mounted on an inclined shaft by an approach based on incompressible LES combined with the VOF method to represent the liquid and vapor phases and the Kunz cavitation model. In their study, LES was demonstrated capable of capturing the mechanisms by comparing the LES results with experimental results. Furthermore, more promising results with refined bubble and vortex structures have been obtained using LES turbulence models to numerically simulate cavitation flows around other objects underwater [15]. To our knowledge, the numerical simulation of an unsteady cavitating flow around a propeller in a non-uniform wake with the use of an explicit LES approach has never been reported in the literature. Detailed results obtained using LES methods to simulate the propeller tip vortex cavitation are particularly limited. Much work is needed for a more comprehensive understanding of this issue. In this study, a numerical simulation of the cavitating flow around a highly skewed propeller in a non-uniform ship wake is performed based on an explicit LES approach with k-μ subgrid model. The Kunz cavitation model, the VOF method, and a moving mesh scheme are also adopted. Experimental [15] and numerical results are compared to prove the validity of the method. Furthermore, an analysis of the factors that affect the cavitation on the propeller is conducted based on the numerical simulation results. Influences between vortex structures and cavity structures are also briefly analyzed.

Getting inspired from the study of Hanshin Seol [27],Chang et al [26], Chahin et al [25], Knud [21] and Arndt et al [23], the present study has numerically investigated the feasibility of the mass injection technique in mitigating sheet and blade root cavitation. The result showed that the compressible fluid is more appropriate than incompressible one, for mass injection approach. Flowing the injecting jet against the upstream, with a radial inclination, has been found very preferable for the effective distribution of injection mass. Moreover, the influence of the profile of rear portion of vessel found to be negligible in vapour formation, which can be a guideline for future analysis.

Keywords

Propeller, CFD, Cavitation, Multi phase flows, Validation.

Methodology

For the computation, the k-ω SST turbulence model with the curvature correction and the Zwart cavitation model have been applied on the commercial CFD Code ANSYS. ANSYS is a 3-D mesh code and solves a set of time-dependent Reynolds-averaged Navier–Stokes equations

(URANS), where an implicit finite volume scheme is applied [28]. The relations among volume fraction, mass and momentum in the scheme are expressed in equation (1) and (2):

$$\frac{\partial \rho_m}{\partial t} + \frac{\partial (\rho_m U_i)}{\partial x_i} = 0 \tag{1}$$

$$\frac{\partial (\rho_m u_i u_j)}{\partial x_j} + \frac{\partial (\rho_m u_i)}{\partial t} = -\frac{\partial P}{\partial x_i} + \frac{\partial}{\partial x_j}\left[\mu_m \left(\frac{\partial u_i}{\partial x_j} + \frac{\partial u_j}{\partial x_i}\right)\right] + \frac{\partial (\tau_{tij})}{\partial x_j} \tag{2}$$

Here, u is velocity, P is pressure and other have their traditional meaning.

Turbulence model: As under adverse pressure gradients and separating flow, the prediction of shear stress transport (SST) k–ω turbulence model is satisfying, the model has been used in many studies [29]. The model is expressed in equation (3).

$$\frac{\partial (\rho k)}{\partial t} + \frac{\partial (\rho k u_i)}{\partial x_i} = \partial \frac{(\Gamma_k \frac{\partial k}{\partial x_j})}{\partial x_j} + \tilde{G}_k - Y_k + S_k \tag{3}$$

Cavitation model: A cavitation process is governed by the mass transfer equations. Equation (4) offers the conservation equation of vapor volume fraction. On the other hand, the conservation equation of gas volume fraction is expressed in equation (5).

$$\frac{\partial (\rho_v \alpha_v)}{\partial t} + \frac{\partial (\rho_v \alpha_v u_i)}{\partial x_i} = \dot{m}^{out} - \dot{m}^{in} \tag{4}$$

$$\frac{\partial (\rho_g \rho_g)}{\partial t} + \frac{\partial (\rho_g \alpha_g u_i)}{\partial x_i} = 0 \tag{5}$$

Here, the symbols have their traditional meaning.

Singhal cavitation model, Merkle model, Schnerr and Sauer model, Zwart model and Kunz model [29] are some of the common cavitation models. Zwart-Gerber-Belamri model is favorable for both mixture and Eulerian multiphase models. The model was validated against experimental data [30]. The mass change rate of a single bubble in Zwart model is expressed in equation (6).

$$R = n \times (4\pi \Re_B^2 \rho_\upsilon \frac{d\Re_B}{dt}) \tag{6}$$

Here, $\Re_B$ = Bubbles Radius, ρ_υ = Vapor Density

The following generalized formulation is used, to apply the equation to the bubble collapse process (condensation):

$$R_e = F \frac{3\alpha \rho_v}{\Re_B} \sqrt{\frac{2}{3} \frac{|P_B - P|}{\rho_l}} sign(P_B - P) \tag{7}$$

In the model the cavitation bubble has considered not to interact with each other, during the formation of the nucleation site of the cavitation bubbles. With the increase of the vapor volume fraction, the nucleation site density must decrease accordingly. Eventually, the final form of this cavitation model is expressed in equation (8) and (9).

If, $P \le P_v$

$$R_e = F_{vap} \frac{3\alpha_{nuc}(1-\alpha_v)\rho_v}{\Re_B}\sqrt{\frac{2}{3}\frac{P_v - P}{\rho l}} \quad (8)$$

If, $P \ge P_v$

$$R_e = F_{cond} \frac{3\alpha_v \rho_v}{\Re_B}\sqrt{\frac{2}{3}\frac{P - P_v}{\rho l}} \quad (9)$$

Here, α_{nuc} = nucleation site volume fraction = 5×10^{-4}, F_{vap} = evaporation coefficient = 50, P = the local far-field pressure, P_v = saturation vapor pressure, F_{cond} = condensation coefficient = 0.001, $\Re_B$ = 10^{-6} m.

The general formula to derive thrust is given as-

$$F = \dot{m}_1 V_1 - \dot{m}_2 V_2 + (P_1 - P_2)A \quad (8)$$

Here, A = cross section area, $\dot{m}$ = mass flow rate, V = flow velocity, P = static pressure. As for the A being constant, the equation (8) can be further modified as-

$$\frac{F}{A} = \rho_1 V_1^2 - \rho_2 V_2^2 + (P_1 - P_2) \quad (9)$$

The equation (9), will be used to draw the thrust profile for effectiveness comparison.

Numerical Model Validation

The model was run in the Fluent software [31]. For the simulation, a 7th generation Core-i5 Desktop, with 8GB RAM, was used to ran the software. At first, the model was validated against an experiment, on the formation of cavitation for cone shaped specimen. The setup consisted of 47357 elements, as the grid view of the setup in Figure 2 showed. The model is justified, as the comparison between the experiment and the computation in *Figure 3* showed negligible error.

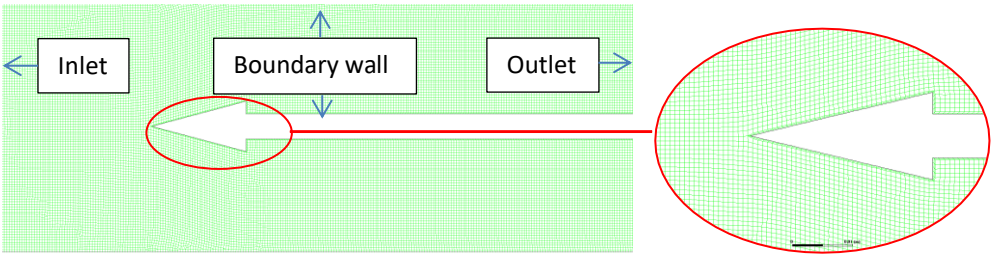

Figure 2: Grid view of dummy setup (left) and the zoom in view of mesh near the cone.

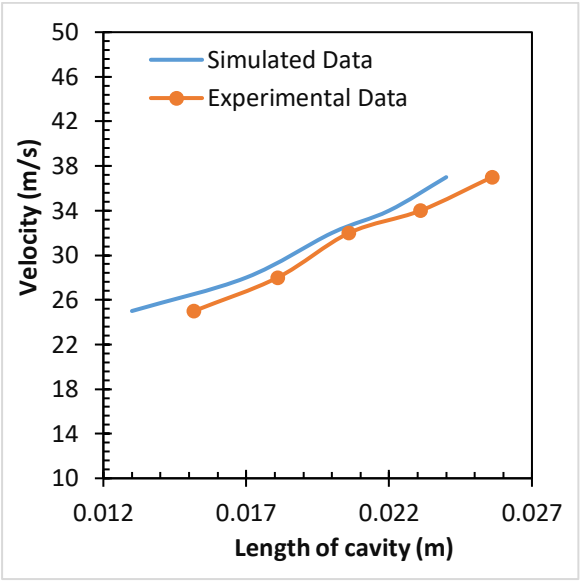

Figure 3: Validation graph

Computational setup

The setup domain is divided into one stator, one rotor. The rotor is a disk with a cavity, with the profile of the propeller geometry, as shown in Figure 4. For the final setup, the INSEAN E779A propeller was modified in the Solidworks designing software and imported to Ansys Design Module [32]. The INSEAN E779A is a popular propeller design and many studies were conducted on this profile [12, 33-35]. For the current study the profile has been modified for simplification. The important dimensions of the modified INSEAN E779a propeller are shown in Table 1. For both inlet and outlet, the initial pressure difference was set to zero. The outer wall was set to pressure outlet. The operating pressure was 101325 Pa. It was assumed that the buoyancy of bodies in water is negligible, no slip condition prevails on the propeller surface and operating fluid is incompressible. To get a fully developed state, primitively the setup was run without water injection, assigning the ports as wall. The rotation of the propeller was increased step-by-step and finally set to 3000rpm. Afterwards, to capture the water injection phenomenon, the boundary condition for the outer ports was changed to pressure inlet. Later on, for different conditions, the setup was further computed. Each time, it took around 12 hours to achieve a stable result.

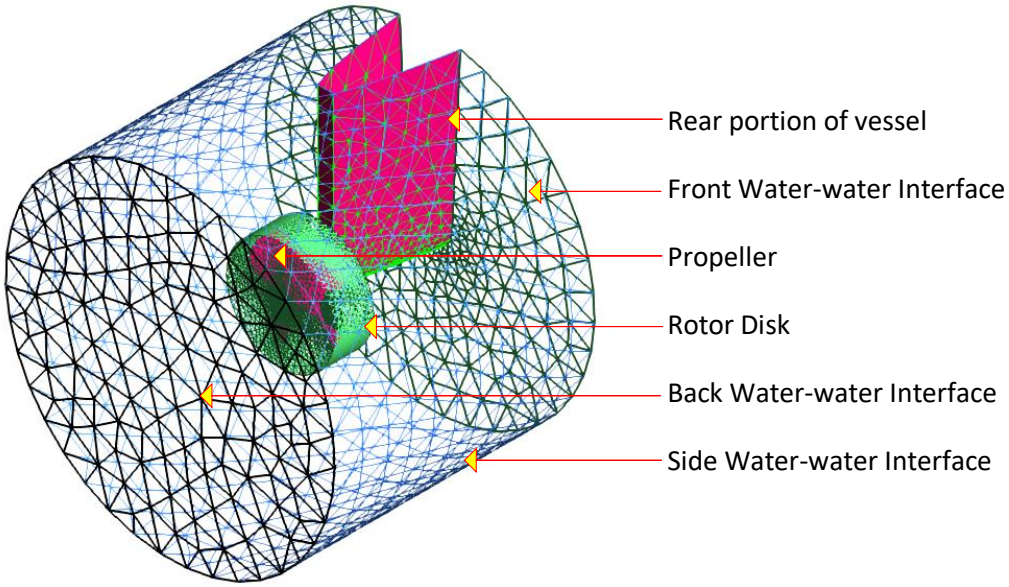

Figure 4: Computational domain

Table 1: Propeller dimensions

Angle of attack (at the tip)	19.2972rad
number of blades	4
skew angle	0^0
rake angle	4.56^0
pitch	250 mm
P/D	1.1
Cupped Angle	0^0
Diameter of the propeller	225mm

Grid Properties

Eight circular ports was drawn on the blades in Solidworks designing software [32]. As shown in Figure 6, four of the ports are close to the shaft (inner-port) and others are near the tip of the blades (outer-port). About the mesh validation, comparison among 2mm, 1.8mm and 1.5mm element sizes near the propeller surface, gave convincing agreement, as shown in Figure 5. Lack of mesh density is one of the reasons for deviations in numerical results [33]. Thus, the element number was set to over a million, where the element size is 1.5mm, near the surface. Unstructured mesh, with inflation criterion, was selected to get optimum mesh quality and smooth blade surface within the specified mesh quantity. The stator mesh size was set comparatively large to reduce element number and cheap computation. The sliding mesh method was selected for the rotating mesh of the rotor.

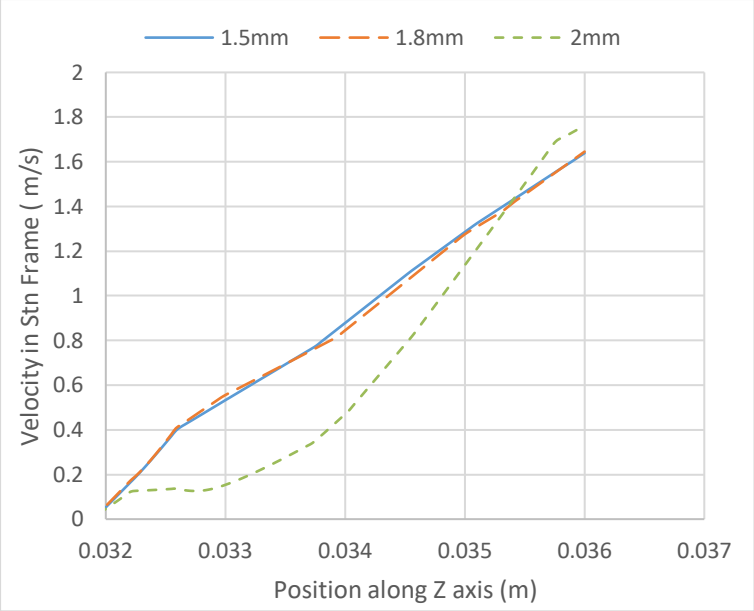

Figure 5: Velocity profile for different mesh sizes.

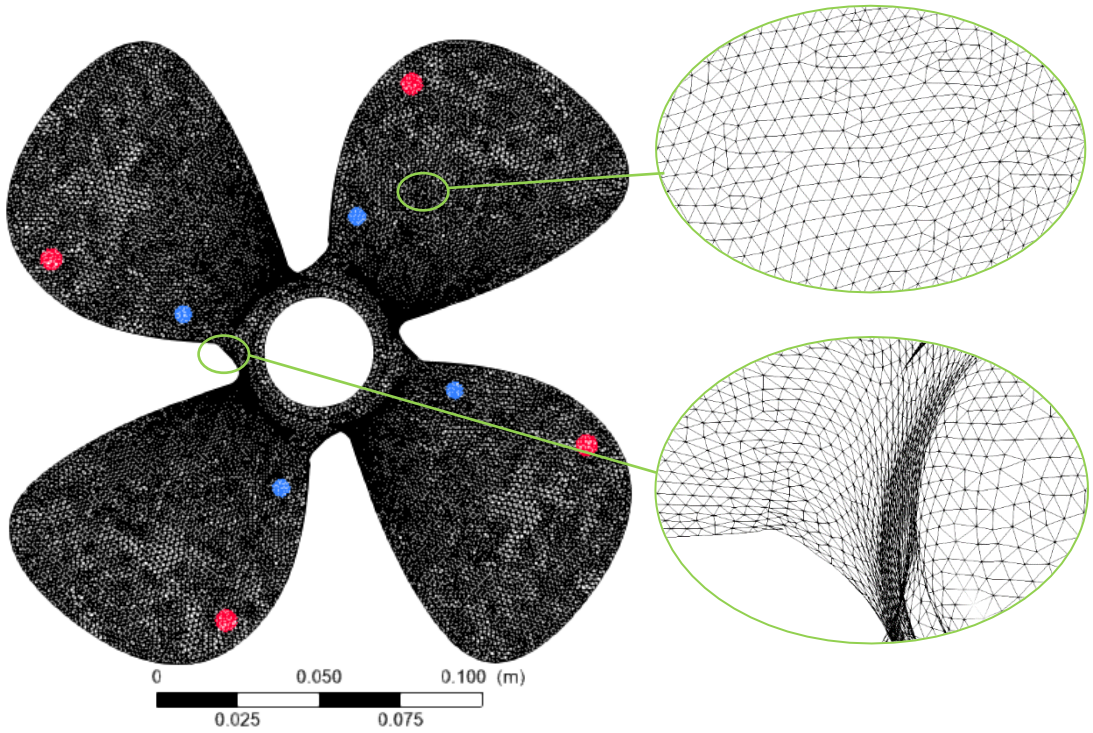

Figure 6: The grid view of the propeller, with inner (blue) and outer ports (red).

Numerical setup

Pressure based solver, with absolute velocity formulation was selected. SST k-omega was chosen for the viscous model. Energy model remained off. For multiphase model mixture model, with three Eulerian phases was selected. Slip velocity and implicit body force were activated. Simple scheme, least square cell based gradient, body force weighted pressure, first order momentum, compressive volume force, first order turbulent kinetic energy, first order

dissipation rate were selected for pressure-velocity coupling. Solution controls were in default. Hybrid initialization was selected for time step of 10^{-5} second and maximum iteration of 2000. After obtaining stability, the time step was set to 10^{-4} second. It took around 5 days, to compute the initial 7 seconds scenario of the setup.

Results and Discussions

Effectiveness of water injection

At first water was injected through the outer ports to increase the pressure of the region where the operating pressure is below vapour pressure of water. As shown in Figure 7, the midchord cavitation has been able to minimize through water injection, for 130000 Pa initial pressure gauge pressure inlet. But, being not an expandable fluid, water cannot effectively diffuse the region to prevent cavity formation. Moreover, the operating pressure being below vapour pressure, water turns into vapour, contributing to cavitation, as shown in Figure 8. The Figure 9 gives more specific view of degree of phase changes throughout the circular line, indicated in red in Figure 8, for both inner port and outer port water injection condition. Moreover, the Figure 10 confirms that water injection has insignificant effect on sheet cavitation, as the circular line covers the region of maximum sheet cavitation.

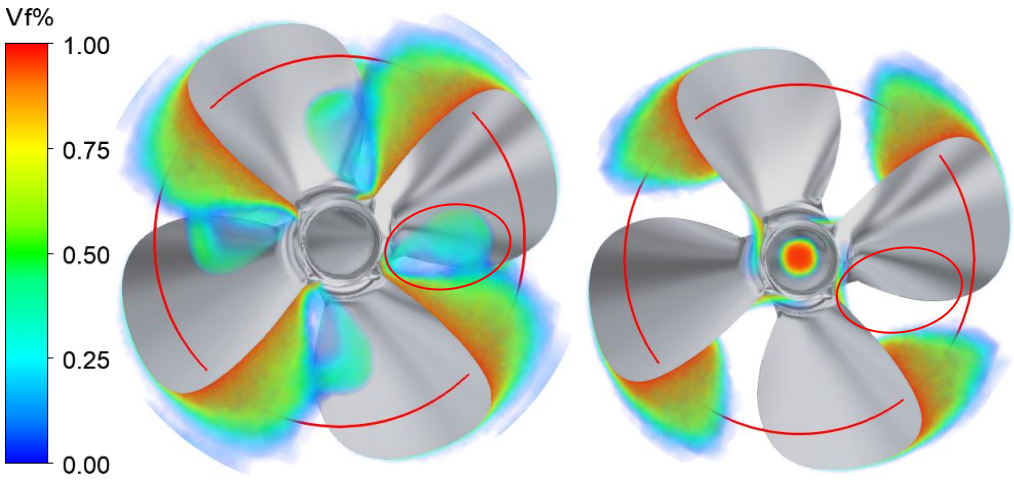

Figure 7: Cavitation cloud with without water injection (left) and injection (right)

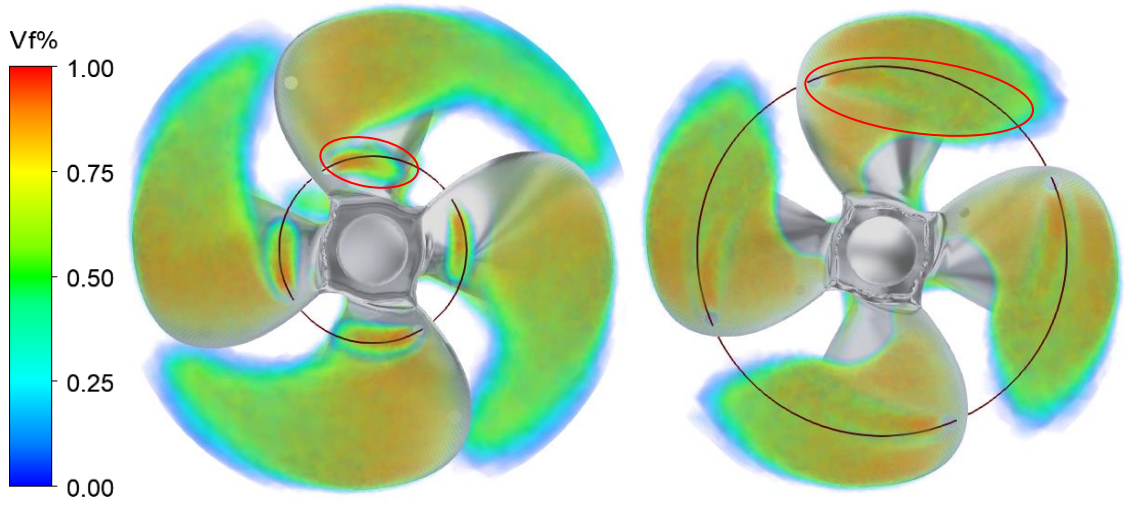

Figure 8: Transformation of injected water into vapour for inner port injection (left) and outer port injection (right).

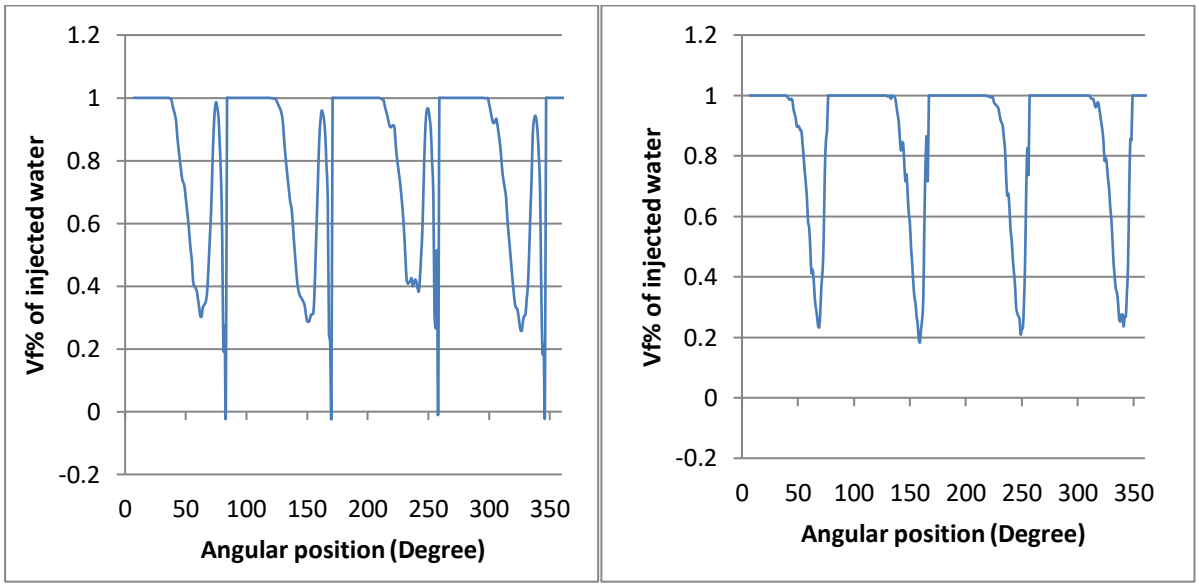

Figure 9: Changes of volume fraction of injected water for inner port (left) and outer port (right) injection.

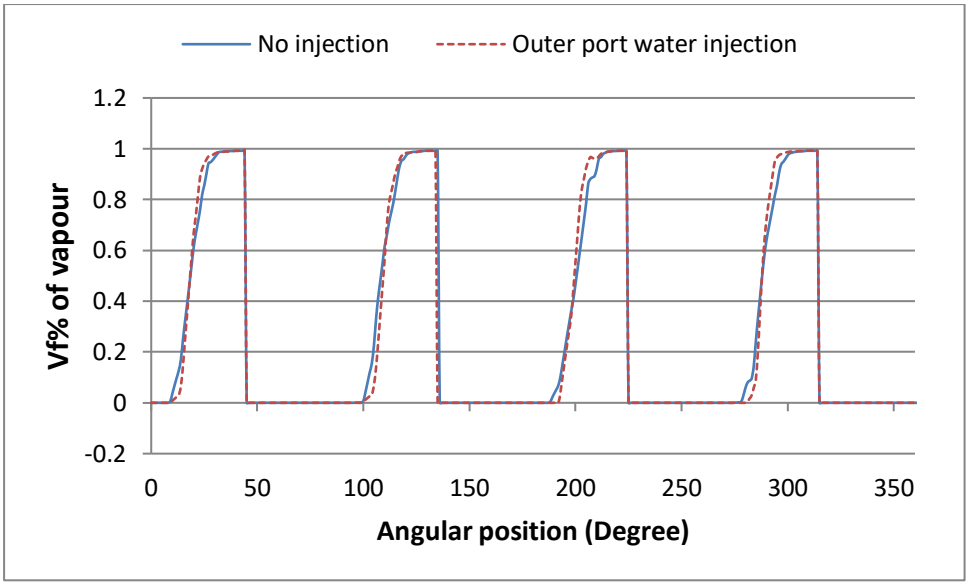

Figure 10: Effectiveness of water injection.

Besides, viscosity and density of water is significant, making it very energy consuming to transfer, especially is Pa pressure inlet condition. Typically at 20^0C water viscosity is 1.002×10^{-3} Kg·s/m and density is 1000 Kg/m^3. Where, air viscosity is 1.8192×10^{-5} Kg·s/m and density is 1.2 Kg/m^{-3}. Taking turbulence flow into account, coefficients to be same for both water and air and using the equation (8), as the summation of power required for viscosity and weight, it is estimated that for the injection hole be a perfectly straight hole, at ideal case the energy required for pumping for water is significant higher than for air. Thus, the air has been selected for further investigation.

$$\dot{w} = \dot{v} f \frac{L}{D} \frac{\rho V^2}{2} + \rho \dot{v} V \qquad (8)$$

Here, $\dot{w}$ is required power, $\dot{v}$ is volume flow rate, f is friction factor, L is pipe length, D is hydraulic diameter and V is flow velocity.

Proper location of injection source

While injecting air through outer ports, it was found that air started to swirl towards the axis, as shown in Figure 11. Thus, it was concluded that the centrifugal force has negligible effect on the injected air and thus the ports should be close to the tips, so that the air can successfully reach to the region, where the pressure is below the water vapour pressure.

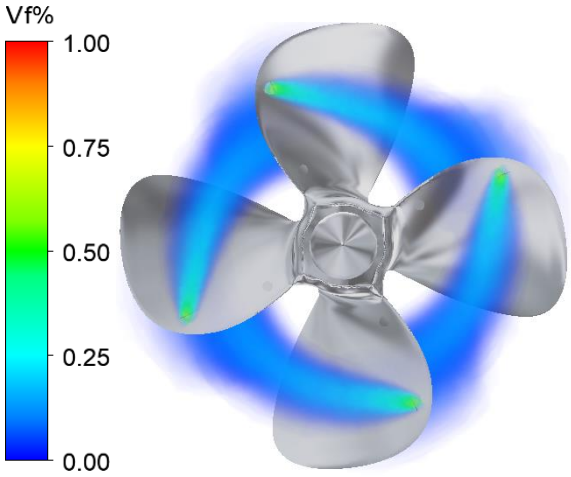

Figure 11: The injected air distribution.

Direction of injection

To find the proper orientation of air injection port only radial and opposite to upstream, with radial inclination criteria have been analysed, for outer port injection. Analysing with 100 m/s air injection, it was found that opposite to upstream, with radial inclination, gave better result with smaller cavitation cloud, as shown in Figure 12. The arrows in Figure 12, indicate the net direction and the net amplitude of injected jet. The result is presented in detail in Figure 13.

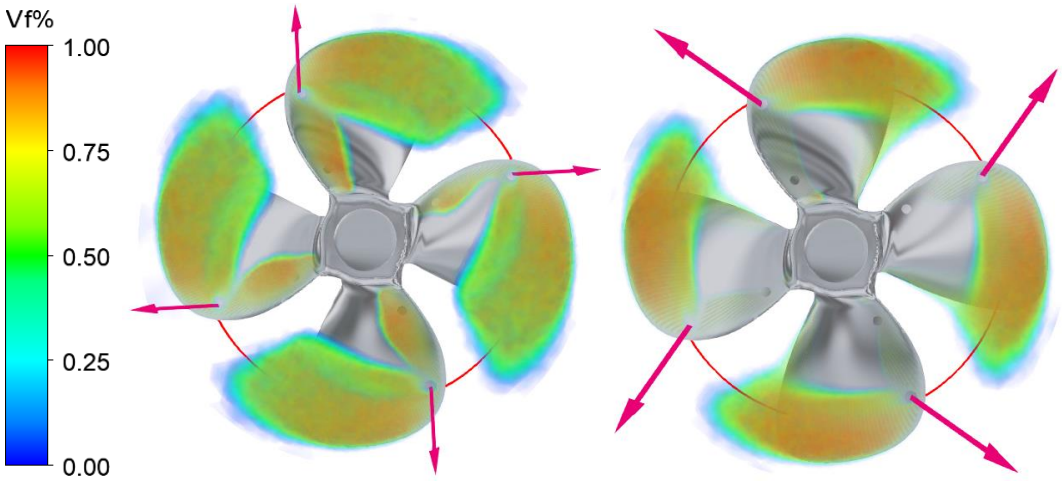

Figure 12: Radial flow (left) amd opposite upstream flow, with radial inclination (right).

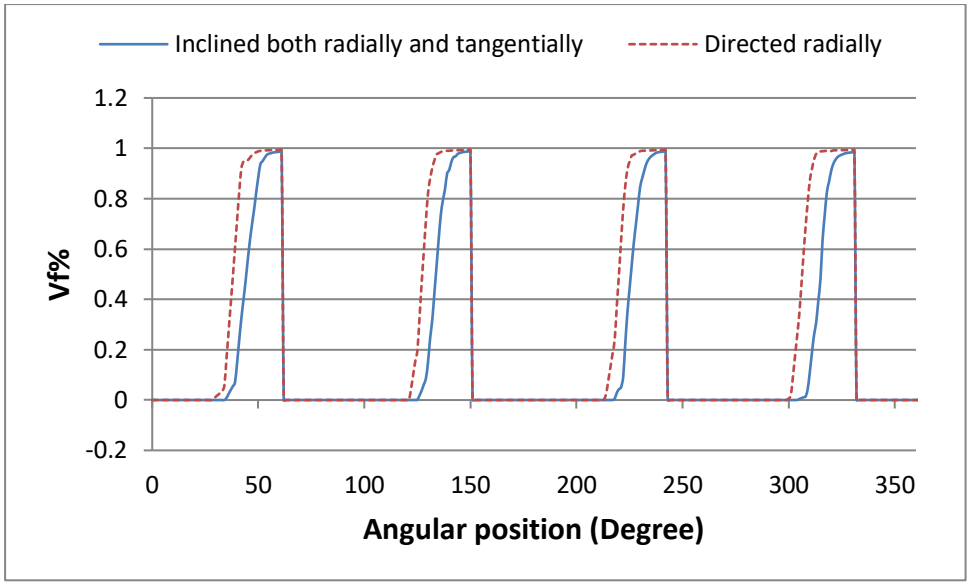

Figure 13: Comparison between radially directed and inclined to both radially and opposite to upstream.

Afterwards, analysis was deducted on the influence of magnitude of the jet, for the both radially and tangentially inclined orientation. The Figure 14 gives the pictorial view of cavitation for 50m/s and 200m/s jet stream, for the mentioned orientation. It was found that the cavitation is mostly reduced for jet stream of 100m/s for 3000rpm, as shown in Figure 15.

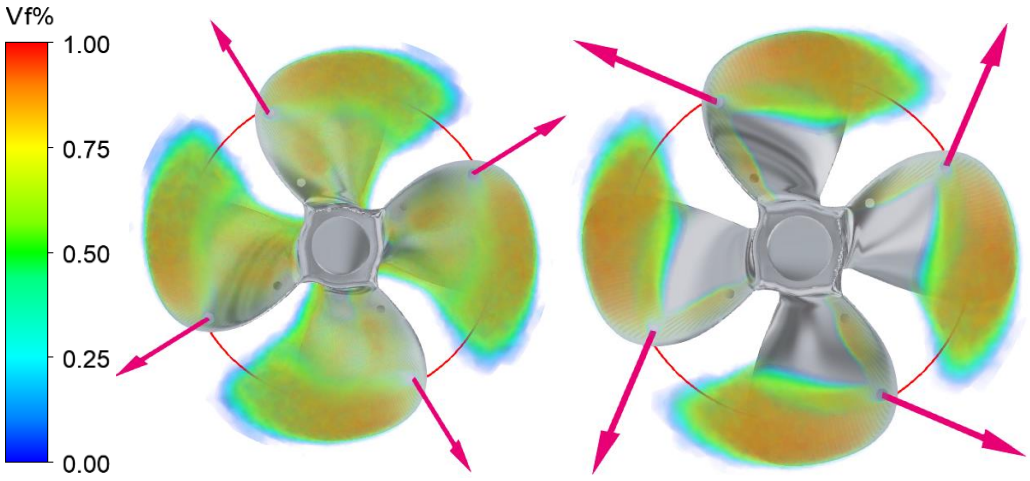

Figure 14: Injection flow rate 50 m/s (left) and 200 m/s (right).

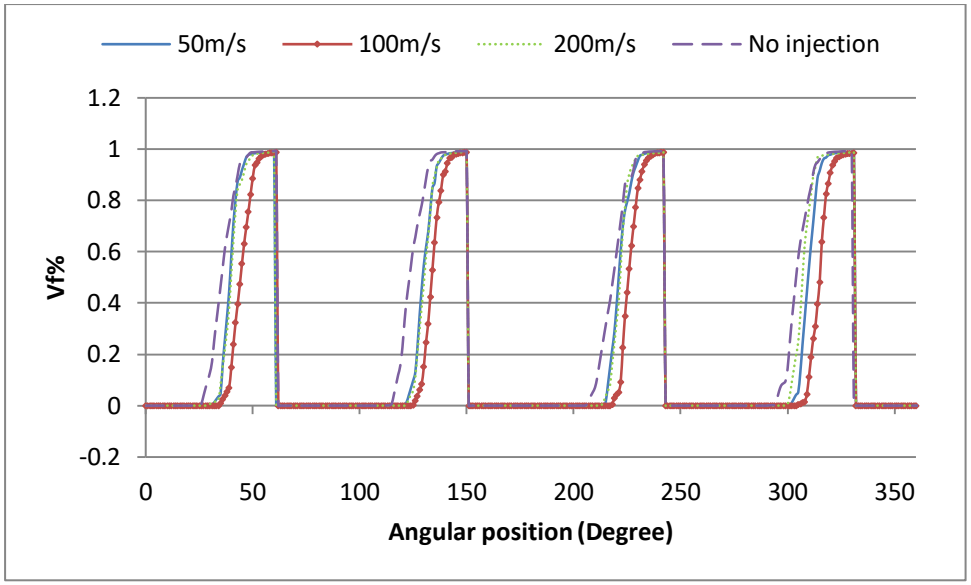

Figure 15: Comparison among different velocities.

It was further found that for this orientation cavitation profile also has negligible effect dramatical changes of initial inlet gauge pressure, ranging from 0 to 101325 Pa, as shown in Figure 16, for 200m/s jet stream at partial radially inclined orientation.

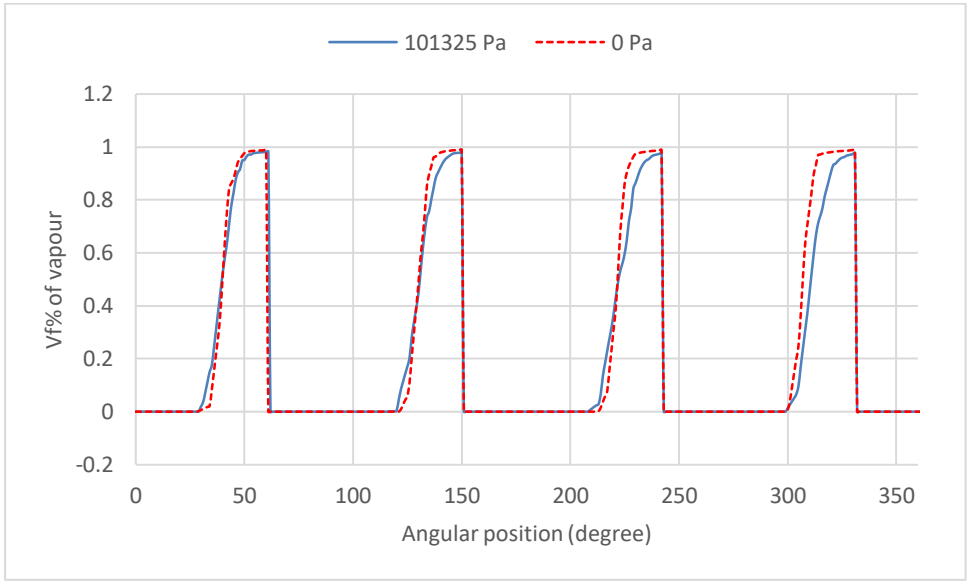

Figure 16: Initial gauge inlet pressure 0 Pa and 101325 Pa.

The Figure 12 and Figure 14 clarify that the midchord cavitation was been properly and effectively eliminated through air injection technique. Moreover, the sheet cavitation babbles were been able to collapse further away from the proceeding blade, which prevents the cavitation to harm the frontal portion of the blades, since the Figure 15 showed the amount of cavitation near the frontal portion of blades is very appreciating for all type air injection conditions, as compared to the no injection condition. From the Figure 17 it is clear that for even some of the worst configurations of air injection, its result is better than air injection.

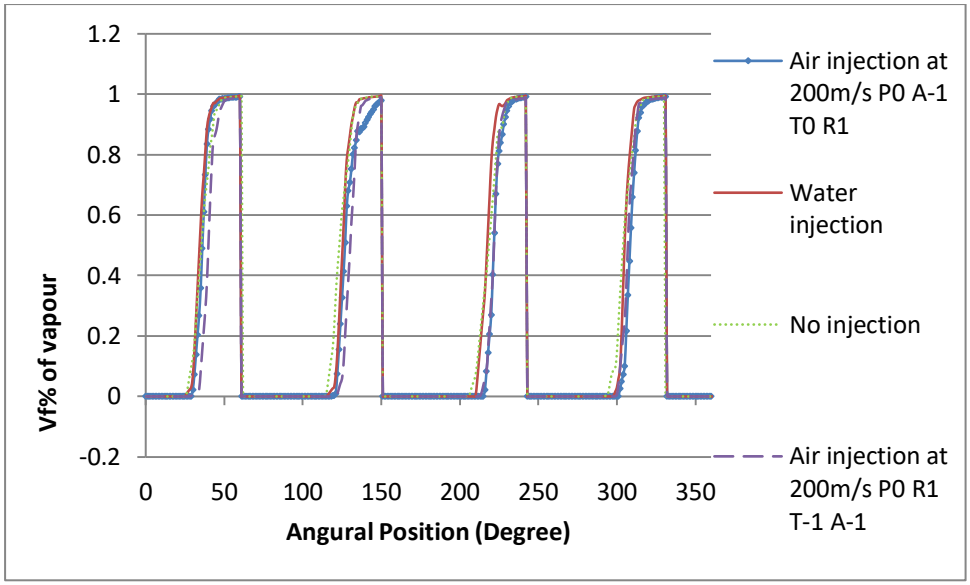

Figure 17: Comparison among air injection, water injection and no injection.

Best configurations

Among the numerical results, four of them were found to be best for the mitigation purpose, as shown in Figure 18 . Among these four, 50m/s P0 T0 R1 A-1 and 100m/s P0 R1 T-1 A-1 are exceptionally better. Moreover, these two are distinct in their direction of injection. The Figure 18 also showed that the water injection even for one of the configuration could not come to close in case of effectiveness. To find out the best configuration, further investigation was conducted on their influence on thrust of the propeller. The thrust profile for a line of (-.372029,0,.15) and (.372029,0,.15) coordinates was been formulated for the two configurations. But as shown in Figure 19, the results gave similar thrust profiles. Thus the two configurations have very negligible difference in their impacts. However, economically one with 50m/s jet stream should be preferred, as it has less energy requirement.

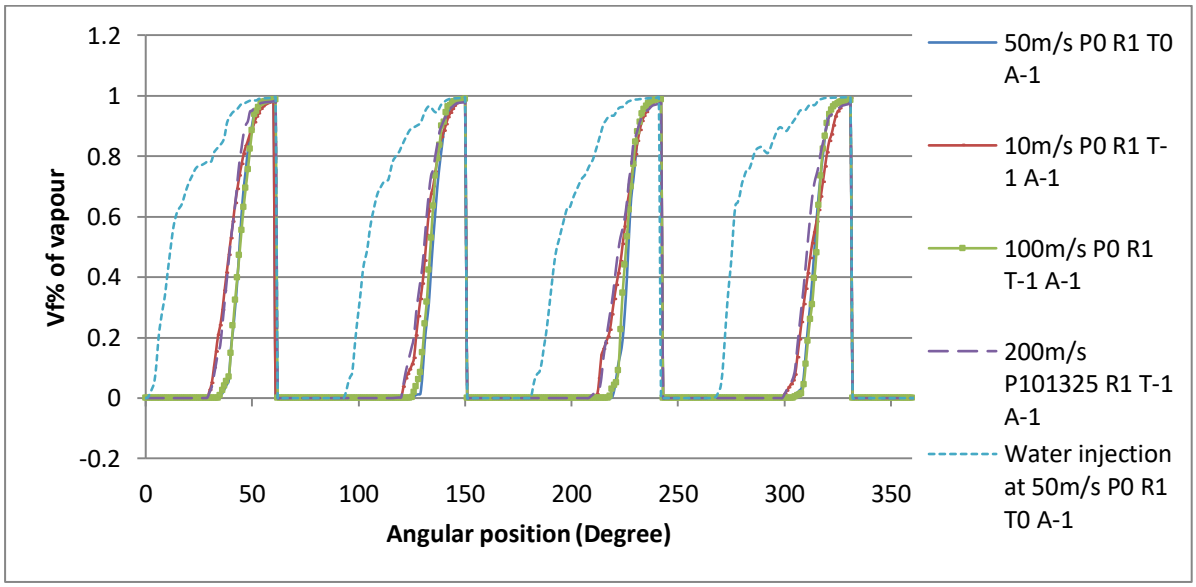

Figure 18: Different configurations for mass injection.

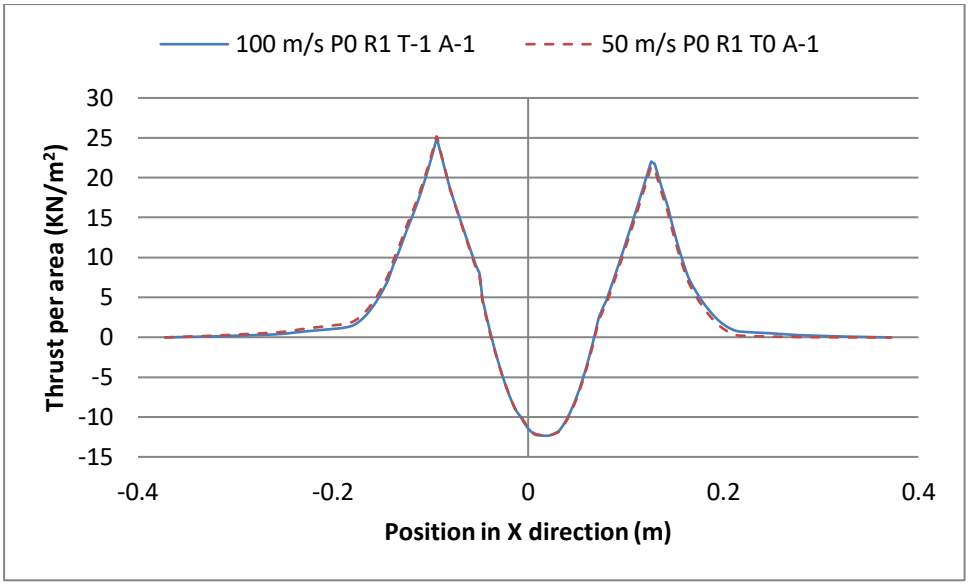

Figure 19: Thrust profile for two configurations.

Influence of rear vessel portion

There was a chance of the obtained result might got deviated by the rear vessel portion profile. Thus, analysis was conducted to check the issue, by taking two different profiles under consideration, as shown in Figure 20. The cavitation cloud patterns for the profiles were given in Figure 21 .The Figure 22 clarifies that the cavitation profile is slightly longer for 2nd cone, than 1st cone. This is might be because the 2nd cone is wider than the 1st, as shown in Figure 23, making more obstacles for upstream water to flow and resulting greater pressure drop. Thus, the cavitation profile pattern may vary for different vessels.

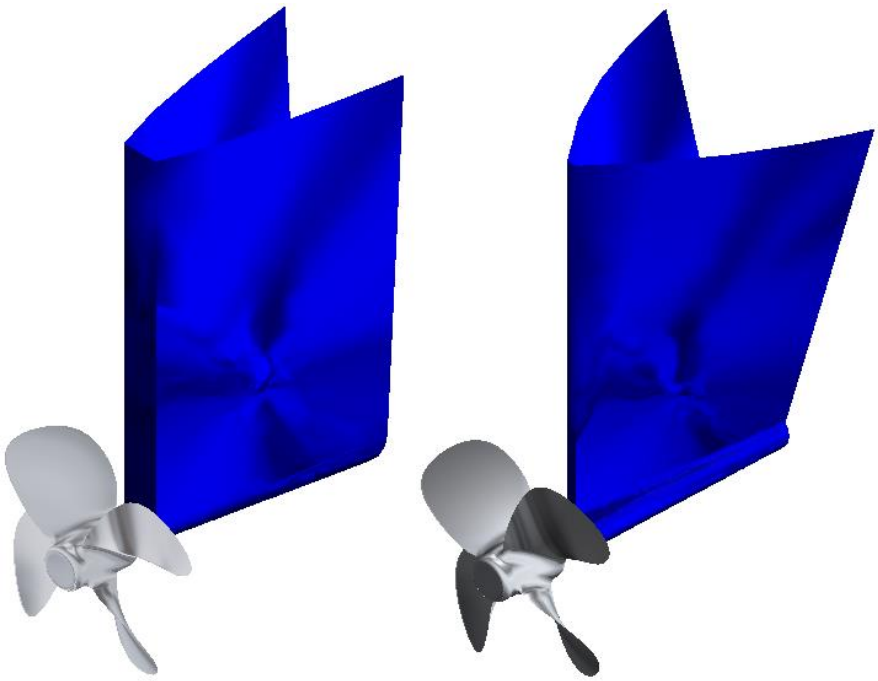

Figure 20: Rear portion profiles, assigned as 1st cone (left) and 2nd cone (right).

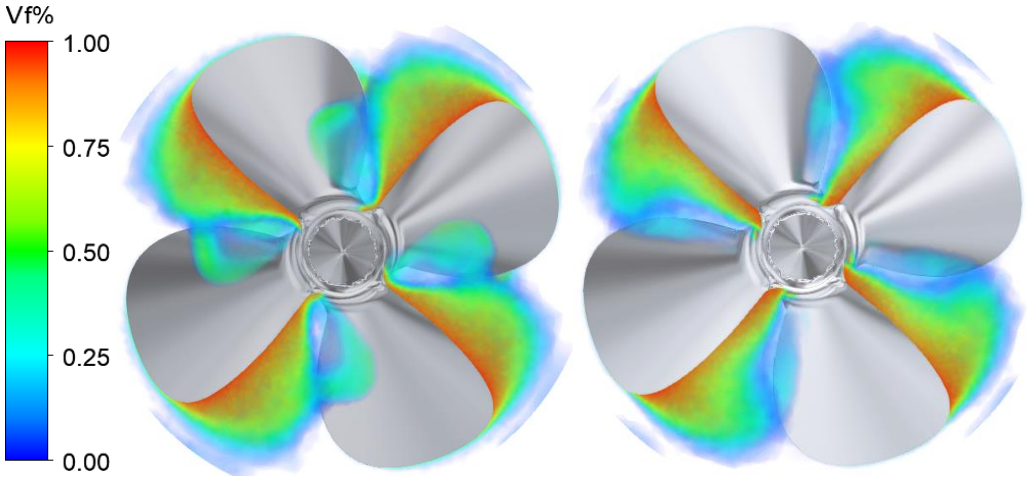

Figure 21: Cavitation for 1st cone (left) and 2nd cone (right).

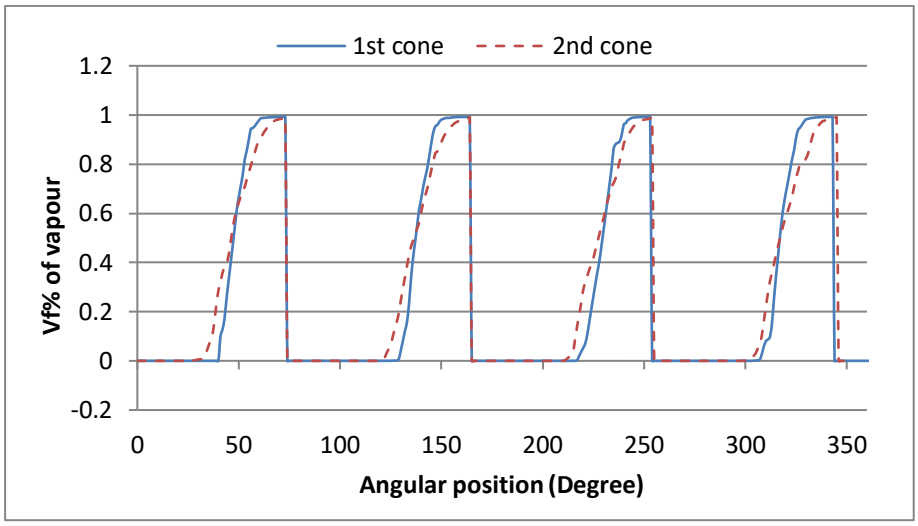

Figure 22: Volume fraction over the circular line for both profiles.

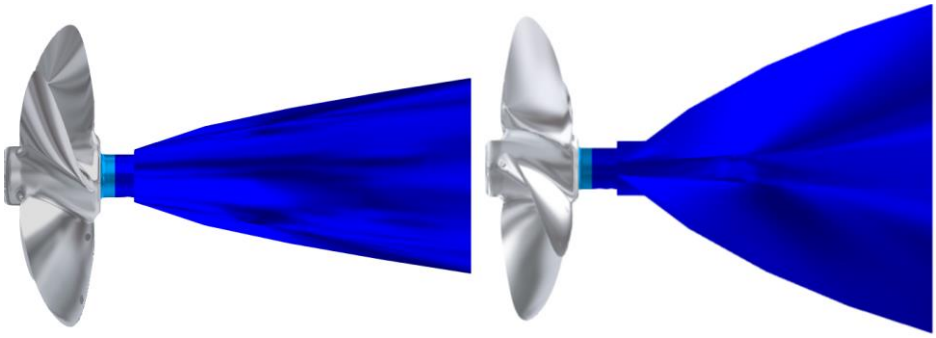

Figure 23: Top view of the 1st cone (left) and 2nd cone (right).

Gratitude

The computer lab of CSE department gave support to carry out the undisturbed long time taking simulation. Besides, the friendly hostel condition was essential in organizing the results and in pondering upon the outcomes. Moreover, the guidelines of lecturer Abdul Karim Sir and Arafat Ahmed Sir, played a demanding role to carry out the study to the end. Most importantly thanks the Lord of existence, for the overall accomplishment of the project.

Conclusion

From the sequential analysis it was found that the air injection approach was better in many aspects over that of water injection. Especially, the sheet, the root cavitation and the midchord cavitation were significantly reduced through the process for the 50m/s P0 R1 T0 A-1 and 100m/s P0 R1 T-1 A-1 configurations. Afterwards, the analysis on the orientation of the injection jet stream showed that the some components of the jet stream should be inclined to the opposite direction of the upstream, to have an effective mass diffusion. Further studies showed that the rear vessel portion profile impacts on the cavitation cloud pattern. Thus, the profile should be in consideration for future numerical studies. Besides, the thinner profile is effective for less formation of cavitation.

Reference

1. Ganz, S. and E. Gutierrez, *Cavitation: Causes, Effects, Mitigation and Application*. 2012, Rensselaer Polytechnic Institute: Hartford, CT, USA.
2. Brennen, C.E., *Cavitation and bubble dynamics*. 2013: Cambridge University Press.
3. Peterson, D.T., *Surface piercing propeller performance*. 2005, Monterey, California. Naval Postgraduate School.
4. Arndt, R., et al., *The singing vortex.* Interface focus, 2015. **5**(5): p. 20150025.
5. Pham, T., F. Larrarte, and D. Fruman, *Investigation of unsteady sheet cavitation and cloud cavitation mechanisms.* Journal of Fluids Engineering, 1999. **121**(2): p. 289-296.
6. Moeny, M., et al. *Cavitation damage from an induced secondary vortex*. in *ASME 2008 Fluids Engineering Division Summer Meeting collocated with the Heat Transfer, Energy Sustainability, and 3rd Energy Nanotechnology Conferences*. 2008. American Society of Mechanical Engineers.
7. Tani, G., M. Viviani, and E. Rizzuto. *Model scale investigation of the effect of different speed reduction strategies on cavitating propeller radiated noise*. in *OCEANS 2015-Genova*. 2015. IEEE.
8. Epps, B.P., O. Víquez, and C. Chryssostomidis, *Dual-operating-point blade optimization for high-speed propellers*. 2011: Sea Grant College Program, Massachusetts Institute of Technology.
9. BAL, Ş., *A method for optimum cavitating ship propellers.* Turkish Journal of Engineering and Environmental Sciences, 2011. **35**(3): p. 319-338.
10. Gaggero, S., J. Gonzalez-Adalid, and M.P. Sobrino, *Design and analysis of a new generation of CLT propellers.* Applied Ocean Research, 2016. **59**: p. 424-450.
11. Yari, E. and H. Ghassemi, *The unsteady hydrodynamic characteristics of a partial submerged propeller via a RANS solver.* Journal of Marine Engineering & Technology, 2015. **14**(3): p. 111-123.
12. Yu, H., et al. *Numerical analysis of cavitation about marine propellers using a compressible multiphase VOF fractional step method*. in *9th Australasian Congress on Applied Mechanics (ACAM9)*. 2017. Engineers Australia.
13. Sakamoto, N., et al. *2015S-GS14-3 CFD Simulations for Cavitating Marine Propellers using Unstructured Cells and Sliding Mesh Technique*. in *Conference Proceedings The Japan Society of Naval Architects and Ocean Engineers*. 2015. The Japan Society of Naval Architects and Ocean Engineers.
14. Gaggero, S., et al., *A study on the numerical prediction of propellers cavitating tip vortex.* Ocean engineering, 2014. **92**: p. 137-161.
15. Yu, C., et al., *Large eddy simulation of unsteady cavitating flow around a highly skewed propeller in nonuniform wake.* Journal of Fluids Engineering, 2017. **139**(4): p. 041302.
16. Yilmaz, N., M. Khorasanchi, and M. Atlar. *An investigation into computational modelling of cavitation in a propeller's slipstream*. in *Fifth International Symposium on Marine Propulsion*. 2017.
17. Hu, J., et al., *Cavitation Simulation of Highly Skewed Propellers.* DEStech Transactions on Engineering and Technology Research, 2017(icaenm).
18. Wu, Q., et al., *Numerical modelling of unsteady cavitation and induced noise around a marine propeller.* Ocean Engineering, 2018. **160**: p. 143-155.
19. Chekab, M.A.F., et al., *Investigation of Different Methods of Noise Reduction for Submerged Marine Propellers and Their Classification.* American Journal of Mechanical Engineering, 2013. **1**(2): p. 34-42.
20. Nwaoha, T.C., S. Adumene, and T.E. Boye, *Modelling prevention and reduction methods of ship propeller cavitation under uncertainty.* Ships and Offshore Structures, 2017. **12**(4): p. 452-460.

21. Thomsen, K., *Mitigation of cavitation effects by means of gas bubbles on a surface.* Journal of nuclear materials, 2006. **356**(1-3): p. 321-324.
22. Lee, J.-H., et al., *Possibility of air-filled rubber membrane for reducing hull exciting pressure induced by propeller cavitation.* Ocean Engineering, 2015. **103**: p. 160-170.
23. Arndt, R., C. Ellis, and S. Paul, *Preliminary investigation of ttie Use of Air Injection to Mitigate Cavitation Erosion.* 1995.
24. Lee, J.-H., et al., *Reduction of propeller cavitation induced hull exciting pressure by a reflected wave from air-bubble layer.* Ocean Engineering, 2014. **77**: p. 23-32.
25. Chahine, G., G. Frederick, and R. Bateman, *Propeller tip vortex cavitation suppression using selective polymer injection.* Journal of fluids engineering, 1993. **115**(3): p. 497-503.
26. Lee, C.-S., et al., *Propeller tip vortex cavitation control and induced noise suppression by water injection.* Journal of Marine Science and Technology, 2018. **23**(3): p. 453-463.
27. Seol, H., *Time domain method for the prediction of pressure fluctuation induced by propeller sheet cavitation: Numerical simulations and experimental validation.* Ocean engineering, 2013. **72**: p. 287-296.
28. Brennen, C.E., *Cavitation and Bubble Dynamics* 1995: Oxford University Press
29. Javadpour, S.M., et al., *Experimental and numerical study of ventilated supercavitation around a cone cavitator.* Heat and Mass Transfer, 2017. **53**(5): p. 1491-1502.
30. *16.7.4 Cavitation Models*. [cited 2018; Available from: http://www.afs.enea.it/project/neptunius/docs/fluent/html/th/node343.htm.
31. *ANSYS*. 2018 8/28/2018]; Available from: https://www.ansys.com/.
32. *SOLIDWORKS 2019 | PROVEN DESIGN TO MANUFACTURE SOLUTION*. 2018 [cited 2018; Available from: https://www.solidworks.com/.
33. Salvatore, F., H. Streckwall, and T. van Terwisga. *Propeller cavitation modelling by CFD-results from the VIRTUE 2008 Rome workshop*. in *Proceedings of the First International Symposium on Marine Propulsors, Trondheim, Norway*. 2009. Citeseer.
34. Bensow, R.E. and G. Bark, *Implicit LES predictions of the cavitating flow on a propeller.* Journal of Fluids Engineering, 2010. **132**(4): p. 041302.
35. Bensow, R.E. and G. Bark. *Simulating cavitating flows with LES in OpenFoam*. in *V European conference on computational fluid dynamics*. 2010.